

Suzaku Studies of the Supernova Remnant CTB 109 Hosting the Magnetar 1E 2259+586

TOSHIO NAKANO¹, HIROAKI MURAKAMI¹, KAZUO MAKISHIMA^{1,2,3}, JUNOKO S. HIRAGA³,
HIDEKI UCHIYAMA⁴, HIDEHIRO KANEDA⁵, AND TERUAKI ENOTO^{6,7} *

¹*Department of Physics, Graduate School of Science, The University of Tokyo 7-3-1 Hongo, Bunkyo-ku, Tokyo 113-0033*

²*MAXI Team, Institute of Physical and Chemical Research (RIKEN) 2-1 Hirosawa, Wako-shi, Saitama 351-0198*

³*Research Center for the Early Universe, The University of Tokyo 7-3-1, Hongo, Bunkyo-ku, Tokyo 113-0033*

⁴*Science Education, Faculty of Education, Shizuoka University 836 Ohya, Suruga-ku, Shizuoka 422-8529*

⁵*Goddard Space Flight Center, NASA, Greenbelt, Maryland, 20771, USA*

⁶*Graduate School of Science, Nagoya University, Chikusa-ku, Nagoya, 464-8602*

⁷*RIKEN Nishina Center, 2-1 Hirosawa, Wako-shi, Saitama 351-0198*

nakano@juno.phys.s.u-tokyo.ac.jp

(Received ; accepted)

Abstract

Ages of the magnetar 1E 2259+586 and the associated supernova remnant CTB 109 were studied. Analyzing the Suzaku data of CTB 109, its age was estimated to be ~ 14 kyr, which is much shorter than the measured characteristic age of 1E 2259+586, 230 kyr. This reconfirms the previously reported age discrepancy of this magnetar/remnant association, and suggests that the characteristic ages of magnetars are generally over-estimated as compared to their true ages. This discrepancy is thought to arise because the former are calculated without considering decay of the magnetic fields. This novel view is supported independently by much stronger Galactic-plane concentration of magnetars than other pulsars. The process of magnetic field decay in magnetars is mathematically modeled. It is implied that magnetars are much younger objects than previously considered, and can dominate new-born neutron stars.

Key words: ISM: supernova remnants — Stars:neutron Stars:magnetar — Stars:magnetic fields —X-rays: individuals:CTB 109, —X-rays: individuals:1E 2259+586

* Last update: October 23, 2014

1. INTRODUCTION

1.1. *Relations between Magnetars and SNRs*

Twenty seven Galactic and Magellanic X-ray sources are thought to constitute a class of objects called magnetars, which are single neutron stars (NSs) with extremely strong magnetic fields of $B = 10^{14-15}$ G. They are believed to shine (mainly in X-rays) consuming the energies in their strong magnetic fields, because their X-ray luminosities exceed their spin-down luminosities and they are not likely to be accreting objects. The magnetar concept well explains other peculiar characteristics of these objects, such as long pulse periods clustered in a narrow range (2 – 11 s), relatively large period derivatives, and unpredictable sporadic burst activities. However, we do not know yet how they are formed and how such strong fields evolved.

Supernova remnants (SNRs) associated with magnetars are expected to provide us with valuable clues to the scenario of magnetar production (e.g., Vink 2008; Safi-Harb & Kumar 2013). As a result, the study of SNR/NS associations (e.g., Seward 1985; Chevalier 2005, 2011) has been re-activated since the concept of magnetar has emerged. Although no clear difference in the explosion energy has yet been found between SNRs with and without magnetars (e.g., Vink & Kuiper 2006), an X-ray metallicity study of the SNR Kes 73, hosting the magnetar 1E 1841-045, led Kumar et al. (2014) to infer that the progenitor of this system had a mass of $\gtrsim 20 M_{\odot}$, where M_{\odot} is the solar mass. Through investigations of several SNR/magnetar associations, Safi-Harb & Kumar (2013) characterized environments that are responsible for the magnetar production, and reinforced the view of rather massive progenitors.

Apart from the progenitor issue, one particularly interesting aspect of magnetars, which can be studied by simultaneously considering the associated SNRs, is their age comparison. Of course, as discussed by Gaensler (2004), the ages of a magnetar and of the associated SNR, estimated independently, must agree for them to be regarded as a true association. However, these two age estimations sometimes disagree even in pairs with very good positional coincidence, including the 1E 2259+586/CTB 109 pair which is the topic of the present paper. This is often called “age problem”. While Allen and Horvath (2004) suspected that the problem arises because an SNR age estimate is affected by the presence of a magnetar, Colpi et al. (2000) instead attributed it to magnetic field decay of magnetars, which can make their characteristic ages much longer than their true ages. After the discovery of SGR 0418+5729 (Rea et al., 2010), a magnetar with a low dipole magnetic field, the field’s decay scenario has become more attractive (Dall’Osso et al., 2012; Igoshev, 2012).

Through X-ray studies of CTB 109, the present paper attempts to address two issues. One is to solve the age problem with the 1E 2259+586/CTB 109 system, and the other is to conversely utilize the result to reinforce the nature of magnetars as magnetically driven NSs. After a brief introduction to the target system (section 2), we describe in section 3 and section 4 recent Suzaku observations of CTB 109, and reconfirm the age problem in the system (section 5). Then, an attempt is made in section 6 to solve it invoking the decay of magnetic fields. Finally, we discuss some implications

for the general view of NSs, including in particular their magnetic evolution. Other topics will be discussed elsewhere, including more detailed X-ray diagnostics of CTB 109, the origin of its peculiar half-moon shape, and characterization of the progenitor.

2. Magnetar 1E 2259+586 and SNR CTB 109

2.1. CTB 109

The Galactic SNR, CTB 109, hosting the central point X-ray source 1E 2259+586, was first discovered by the Einstein Observatory (Gregory & Fahlman, 1980) as an extended X-ray source with a peculiar semi-circular shape. It was independently identified as a shell-type SNR by radio observations at 610 MHz (Hughes et al., 1981). A 10 GHz radio map taken with the Nobeyama Radio Observatory revealed good positional coincidence between the radio and X-ray shells, while detected no significant enhancement from 1E 2259+586 (Sofue et al., 1983).

Through CO molecular line observations, Heydari-Malayeri et al. (1981), Tatematsu et al. (1985), and Tatematsu et al. (1987) found a giant molecular cloud located next to CTB 109, and suggested that it may have disturbed the SNR on the west side. Sasaki et al. (2004) conducted a comprehensive X-ray study of this SNR with XMM-Newton. Assuming a distance of $D = 3.0$ kpc (Kothes et al., 2002; Kothes & Foster, 2012), they estimated the shock velocity, age, and the explosion energy as $v_s = 720 \pm 60$ km s⁻¹, 8.8 kyr, and $(7.4 \pm 2.9) \times 10^{50}$ erg respectively. Strong evidence for an interaction between the SNR shock front and the CO cloud was found by using ¹²CO, ¹³CO and Chandra observations (Sasaki et al., 2006). Furthermore, gamma-ray emission was detected with the Fermi-Lat from CTB 109 (Castro et al., 2012). Finally, using Chandra, Sasaki et al. (2013) detected emission from the ejecta component and refined the age as 14 kyr.

2.2. 1E 2259+586

The compact object 1E 2259+586 was first detected in X-rays nearly at the center of CTB 109 (Gregory & Fahlman, 1980). It was soon found to be a pulsar, and the pulse period was at first considered as $P = 3.49$ s (Fahlman et al., 1982). This was due to the double-peaked pulse profile, and the fundamental period was soon revised to $P = 6.98$ s (Fahlman & Gregory, 1983). Repeated X-ray observations enabled the spin down rate to be measured as $\dot{P} = (3 - 6) \times 10^{-13}$ ss⁻¹ (Koyama et al., 1987; Hanson et al., 1988; Iwasawa et al., 1992), and these results made it clear that the spin-down luminosity of 1E 2259+586 (5.6×10^{31} erg s⁻¹) is far insufficient to explain its X-ray luminosity, 1.7×10^{34} erg s⁻¹. Due to this and the long pulse period, 1E 2259+586 was long thought to be an X-ray binary with an orbital period of ~ 2300 s (e.g. Fahlman et al. 1982), and extensive search for a counterpart continued (Davies et al., 1989; Coe & Jones, 1992; Coe et al., 1994). However, no counterpart was found (Hulleman et al., 2000), and instead, tight upper limits on the orbital Doppler-modulation have been obtained as $a_x \sin i < 0.8$ light-s (Koyama et al., 1989), $a_x \sin i < 0.6$ light-s (Mereghetti et al., 1998), and $a_x \sin i < 0.028$ light-s (Baykal et al., 1998). Here, a_x is the semi-major axis of the pulsar's orbit, and i is the orbital inclination. These strange properties of 1E 2259+586 led

this and a few other similar objects to be called Anomalous X-ray Pulsars (AXPs).

In the 1990's, several attempts were made to explain 1E 2259+586 without invoking a companion: e.g., massive white dwarf model (Usov, 1994), and precessing white dwarf model (Pandey, 1996). Monthly observations of 1E 2259+596 over 2.6 years with RXTE gave phase-coherent timing solutions indicating a strong stability over that period (Kaspi et al., 1999). This favored non-accretion interpretation. Heyl & Hernquist (1999) suggested that spin-down irregularities of AXPs are statistically similar to glitches of radio pulsars. Meanwhile, the concept of magnetar was proposed to explain Soft Gamma Repeaters (SGRs) as magnetically-powered NSs, namely, magnetars (Duncan & Thompson, 1992; Thompson & Duncan, 1995). Furthermore, like SGRs, 1E 2259+586 showed an X-ray outburst (Kaspi et al., 2002; Gavriil et al., 2004; Woods et al., 2004). Today, AXPs including 1E 2259+586, as well as SGRs, are both considered to be magnetars. Employing the canonical assumption of spin down due to magnetic dipole radiation, the measured pulse period of $P = 6.98$ s (Iwasawa et al., 1992), and its derivative, $\dot{P} = 4.8 \times 10^{-13} \text{ss}^{-1}$ (e.g., Gavriil & Kaspi 2002), give a dipole magnetic field of 5.9×10^{13} G and a characteristic age of $\tau_c = P/2\dot{P} = 230$ kyr.

3. OBSERVATIONS AND DATA REDUCTION

The Suzaku observations of 1E 2259+586 and CTB 109 were made on two occasions. The first of them was conducted on 2009 May 25 as a part of the AO4 Key Project on magnetars (Enoto et al., 2010). The three cameras (XIS0, XIS1, and XIS3) of the X-ray Imaging Spectrometer (XIS) onboard Suzaku were operated in 1/4-window mode with a time resolution of 2 s (Koyama et al., 2007), to study the 6.98 s pulsation. The rectangular ($17' \times 4'.3$) fields of view of the 1/4-window were center on this magnetar, while the SNR was partially covered. As the second observation, we performed new four pointings onto CTB 109 with Suzaku (PI:T.Nakano) on 2011 December 13. In order to synthesize a whole image of the SNR, all XIS cameras were operated in full-window mode under the sacrifice of time resolution. A log of these observations is given in Table 1.

In the present work, we use the XIS data which were prepared with version 2.7.16.31 pipeline proceeding, and the calibration data updated in January 2013. The data of the Hard X-ray Detector (HXD) from neither observation are utilized here, since the Suzaku data analysis in the present paper focuses on CTB 109, rather than the central magnetar. The data reduction was carried out using the HEADAS software package version 6.13, and spectral fitting was performed with `xspec` version 12.8.0. The redistribution matrix files and the auxiliary response files of the XIS were generated with `xisrmfgen` and `xissimarfgen` (Ishisaki et al., 2007) respectively.

4. DATA ANALYSIS AND RESULT

4.1. Image Analysis

Figure 1 shows a gray-scale mosaic image of CTB 109 obtained with the Suzaku XIS, shown after subtracting non X-ray background. The magnetar, 1E 2259+586, appears as a bright source at

Table 1. Log of Suzaku observations of CTB 109.

Observation ID	α	δ	Start Time	Exposure(ks)
404076010	23 ^h 01 ^m 04 ^s .08	58°58'15".6	2009-05-25 20:00:17	122.6
506037010	23 ^h 01 ^m 06 ^s .96	59°00'50".4	2011-12-13 06:48:41	40.8
506038010	23 ^h 00 ^m 26 ^s .88	58°44'13".2	2011-12-14 04:47:02	41.4
506039010	23 ^h 03 ^m 06 ^s .96	58°58'51".6	2011-12-15 01:57:25	30.4
506040010	23 ^h 03 ^m 06 ^s .96	58°40'51".6	2011-12-15 18:03:52	30.5

the center. The crisscross region including 1E 2259+586 was taken in the first observation, while four square regions represent those from the second one. Thus, the mosaic XIS image reconfirms the half-moon like morphology of this SNR (section 2.1).

As mentioned in section 2.1, the lack of western part of CTB 109 is usually attributed to its interactions with giant molecular clouds. Bright regions in the SNR are also thought to be the signature of such an interaction (Sasaki et al., 2006). These issues, together with detailed spatial distributions of X-ray spectral properties, will be postponed to another publication. The present paper instead deals with average X-ray spectra, because our prime motivation is to estimate the age of CTB 109.

4.2. Spectral Analysis

Figure 2 shows XIS0, XIS1 and XIS3 spectra of CTB 109 from the second observation, extracted from the regions indicated in figure 1 as “NE” and “SE”, which represent two eastern pointing positions. Since these eastern parts of the SNR has kept smooth round shape, the effect from the interaction with GMC seems to be small. Background spectra were extracted from source free regions in the same observation which are also indicated as “BGD” in figure 1. Spectral bins were summed up to attain a minimum of 30 counts bin⁻¹. The “NE” and “SE” spectra are very similar and both exhibit emission lines due to highly ionized atoms such as Ne-IX triplet (~ 0.92 keV), Ne-X Ly α (1.02 keV), Mg-XI triplet (~ 1.35 keV), Si-XIII triplet (~ 1.87 keV), and S-XV triplet (~ 2.45 keV).

We first applied a variable-abundance non-equilibrium ionization (VNEI) plasma emission model to the NE spectra in figure 2 (a). However, even when abundances of Ne, Mg, Si and S are allowed to vary freely, the reduced χ^2 of the fit was not made lower than 1.5. Thus, the single temperature VNEI model was rejected. Other plasma models in `xspec`, such as `vpshock` and `vmekal` were also unsuccessful.

Then, we considered that the SNR emission consists of two components including ejecta and shocked inter-stellar medium (ISM), and added a non-equilibrium ionization (NEI) plasma emission model to model shocked ISM component. Abundances of ISM component was fixed to solar to reduce the number of free parameters.

By introducing this two-component emission model, the fit was improved to $\chi^2/\nu = 1.28$. Since different XIS cameras gave discrepant fit residuals around Mg-XI K α and Si-XIII K α lines,

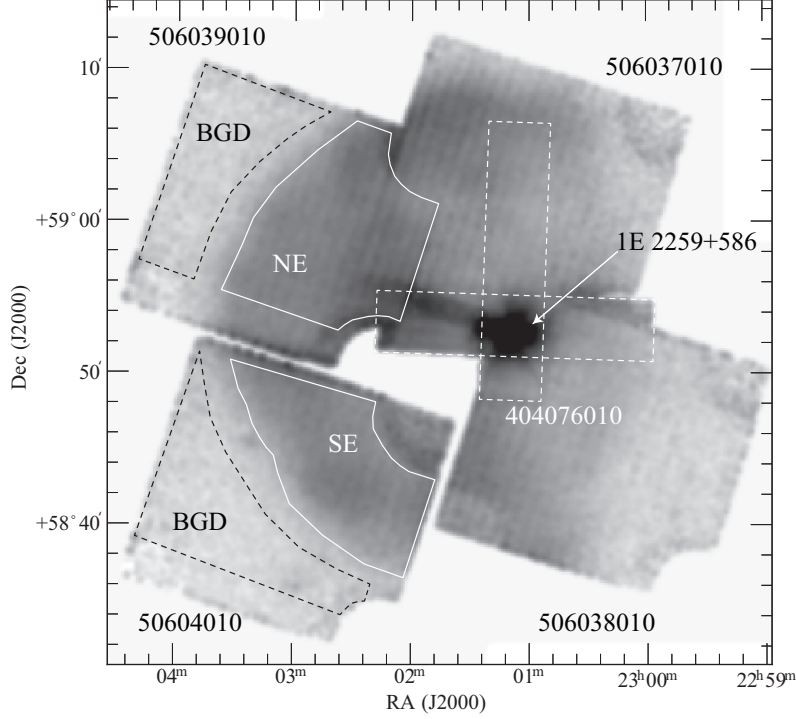


Fig. 1. A mosaic image of CTB 109 obtained in 0.4–5.0 keV with the Suzaku XIS. After subtracting the non X-ray background, the image was corrected for exposure and vignetting. The on-source and background regions are indicated by white and dashed black lines, respectively. Some corners of the square XIS fields of view are masked to remove calibration isotopes.

presumably due to calibration uncertainties of the XIS, we allowed gain parameters of the XIS cameras to vary. Then, the fit has become acceptable with $\chi^2/\nu = 1.06$ (1293/1223). The obtained best-fit parameters are shown in table 2, while the gain parameters in table 3. Since the obtained abundances of the second (Plasma 2) component are all consistent with 1 solar, it is also likely to be dominated by the ISM. The two components are both inferred to be somewhat deviated from ionization equilibrium. The fit was not improved even when the abundance of the Plasma 2 component is allowed to change from 1.0. Similarly, we analyzed the SE spectra shown in figure 2 (b), and derived the parameters which are again summarized in table 2. Thus, the two temperatures are in good agreement between the two regions, although the SE region gives somewhat higher metal abundances. This two-component emission model was also employed by Sasaki et al. (2013).

5. Estimation of the Age of CTB 109

Now that the average plasma properties of CTB 109 have been quantified, let us proceed to our prime goal of studying this SNR, i.e., its age estimation. First, the physical radius of CTB 109 is estimated as $R = (16 \pm 1)d_{3.2}$ pc, from its angular size of $\sim 16'$ and the estimated distance $D = 3.2 \pm 0.2$ kpc (Kothes & Foster, 2012). Here, $d_{3.2} = D/3.2$ is scale factor of distance. Next,

Table 2. Best-fit spectrum parameters for the NE and SE regions*.

Component	Parameter	NE	SE
Absorption	N_{H} (10^{22} cm $^{-2}$)	0.78 ± 0.01	$0.73^{+0.01}_{-0.02}$
Plasma 1 (VNEI)	kT_1	$0.62^{+0.04}_{-0.01}$	$0.65^{+0.02}_{-0.01}$
	η_1^* (10^{12} cm $^{-3}$ s)	$0.37^{+0.05}_{-0.04}$	$0.22^{+0.05}_{-0.06}$
	Ne (solar)	0.8 ± 0.2	$0.8^{+0.2}_{-0.1}$
	Mg (solar)	$0.88^{+0.01}_{-0.06}$	1.1 ± 0.1
	Si (solar)	1.2 ± 0.1	$1.7^{+0.1}_{-0.3}$
	S (solar)	1.0 ± 0.1	$1.7^{+0.2}_{-0.3}$
	Fe (solar)	$0.99^{+0.05}_{-0.06}$	$1.0^{+0.2}_{-0.1}$
	K_1^\dagger (10^{-2} cm $^{-5}$)	$3.7^{+0.2}_{-0.1}$	1.2 ± 0.1
Plasma 2 (NEI)	kT_2	0.26 ± 0.01	0.25 ± 0.01
	η_2^* (10^{12} cm $^{-3}$ s)	> 1	> 1
	Abundance (solar)	1 (fixed)	1 (fixed)
	K_2^\dagger (10^{-2} cm $^{-5}$)	$19.6^{+0.8}_{-1.4}$	$13.2^{+0.8}_{-1.6}$
χ^2/dof		1294/1223	1138/951

*Uncertainties are statistical errors at 90 % confidence.

* Ionization parameter, defined as $\eta = n_e t$

† Normalization of NEI or VNEI, defined as $K = \frac{10^{-14}}{4\pi D^2} \int n_e n_{\text{H}} dV$

Table 3. The best-fit gain parameters*.

region	instrument	slope	offset (eV)
NE	XIS0	0.997 ± 0.001	-5.3 ± 0.2
	XIS1	1.004 ± 0.001	-3.0 ± 0.3
	XIS2	0.986 ± 0.001	-7.0 ± 0.4
SE	XIS0	1.003 ± 0.001	-10.6 ± 0.1
	XIS1	0.993 ± 0.001	6.6 ± 0.1
	XIS2	0.985 ± 0.001	6.6 ± 0.2

*Uncertainties are statistical errors at 90 % confidence.

CTB 109 may be considered in the Sedov phase (neglecting the missing western part). Then, applying the Sedov-Taylor similarity solution (Sedov, 1959; Taylor, 1950) to this SNR, its age can be obtained as

$$\tau_{\text{SNR}} = \frac{2 R}{5 v_s} \quad (1)$$

where v_s again represents the shock front velocity.

Assuming the strong shock limit, we can calculate v_s from the post-shock temperature T_{ps} as

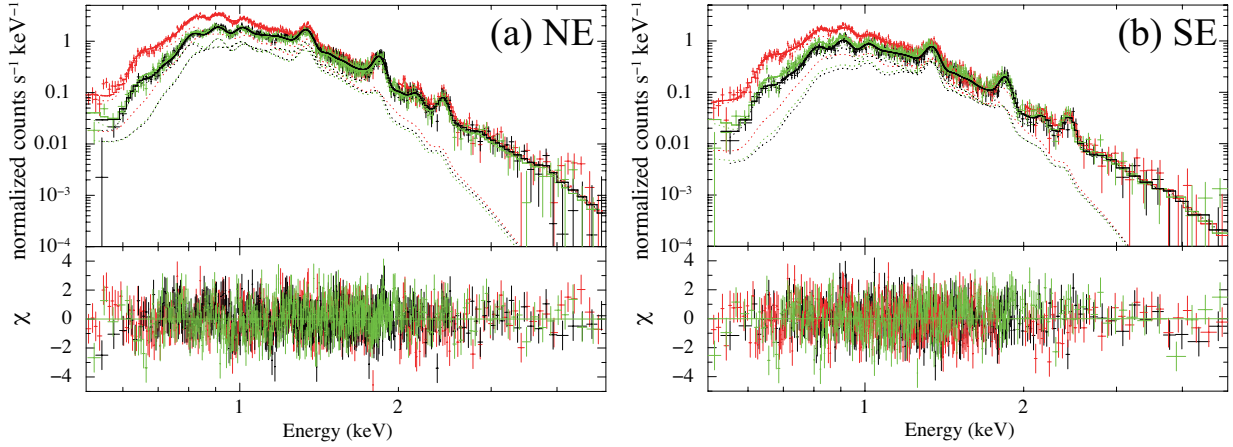


Fig. 2. Background-subtracted XIS0 (black), XIS1 (red) and XIS3 (green) spectra of CTB 109, extracted from the NE (panel a) and SE (panel b) regions. They are fitted simultaneously with a two-component model described in the text. The dotted lines indicate individual model components, with the three colors specifying the three cameras.

$$v_s = \sqrt{\frac{16}{3\bar{m}} kT_{\text{ps}}} \quad (2)$$

where k and \bar{m} , respectively represent the Boltzmann constant and the mean mass per free particle. Assuming a solar abundance (section 4.2), we employed $\bar{m} \simeq 0.61 m_p$ where m_p is the proton mass. Since CTB 109 is a middle-aged SNR without too strong shocks, the electron temperature of the NEI component measured in section 4 can be considered to be close to the kinematic ISM temperature, and hence to T_{ps} (Ghavamian et al., 2007). Thus, substituting 0.25 ± 0.02 keV for T_{ps} , equation (2) gives $v_s = 460 \pm 40$ km s⁻¹, and then equation (1) yields $\tau_{\text{SNR}} \simeq (14 \pm 2)d_{3.2}$ kyr in agreement with Sasaki et al. (2013). Compared to the estimated τ_{SNR} , the characteristic age of 1E 2259+586, $\tau_c = 230$ kyr (section 2.2), is ~ 16 times larger.

If we assume that CTB 109 is in cooling phase rather than Sedov phase, the time dependence of the radius becomes $R \propto t^{2/7}$ (McKee & Ostriker, 1977). Then, the age estimation slightly changes to

$$\tau_{\text{SNR}} = \frac{2R}{7v_s}, \quad (3)$$

and $\tau_{\text{SNR}} = (10 \pm 1)d_{3.2}$ kyr is obtained. Therefore the age discrepancy still persists (even increases).

Let us cross-check the above estimates using the parameter $\eta \equiv n_e t$ (table 2) of the ejecta component. We assume that the SNR has a half spherical shell with thickness of $\Delta R = R/12$ (assuming $4/3\pi R^3 n_0 m_p = 4\pi R^2 \Delta R n_0 m_p$), and the ISM component corresponding to Plasma 2 in table 2 is emitted from this shell. Furthermore, as a simplest approximation, the ejecta component (Plasma 1 in table 2) may be assumed to uniformly fill the inner region, considering that the reverse shock has reached the center of the SNR. In the NE region, the extracted emission volumes of Plasma 1 (ejecta) and Plasma 2 (ISM) can be obtained numerically as $V_1 = 4.0 \times 10^{58} d_{3.2}^3$ cm³ and $V_2 = 1.4 \times 10^{58} d_{3.2}^3$ cm³, respectively. Then, the spectrum normalizations in table 2 give

the averaged density of the ejecta as $n_1 = (0.33 \pm 0.03)d_{3.2}^{-1/2} \text{ cm}^{-3}$ and that of the ISM-shell as $n_2 = (1.2 \pm 0.1)d_{3.2}^{-1/2} \text{ cm}^{-3}$. The time required for the ejecta to become ionized as we now observe is hence estimated as $\eta/n_1 = (29 - 34)d_{3.2}^{1/2} \text{ kyr}$. Applying the same argument to the SE region having the emission volumes of $V_1 = 6.7 \times 10^{57} d_{3.2}^3 \text{ cm}^3$ and $V_2 = 3.3 \times 10^{57} d_{3.2}^3 \text{ cm}^3$, we obtain $n_1 = (0.46 \pm 0.05)d_{3.2}^{-1/2} \text{ cm}^{-3}$ and $n_2 = (0.55 \pm 0.06)d_{3.2}^{-1/2} \text{ cm}^{-3}$, and $\eta/n_1 = (11 - 19)d_{3.2}^{1/2} \text{ kyr}$. Pre-shock density is estimated as $n_0 = n_2/4 = (0.1 - 0.3)d_{3.2}^{-1/2} \text{ cm}^{-3}$. Even though these estimates of τ_{SNR} must have a certain range of systematic uncertainties, large discrepancies significantly remain between τ_{SNR} and τ_c . In fact, it would be difficult to think that CTB 109 are emitting X-rays even at an age of 230 kyr while keeping the regular shape (except the missing western half), because its density environment as estimated is quite typical of a solar neighborhood. Thus, we reconfirm the previously reported age discrepancy (Sasaki et al., 2013) between CTB 109 and 1E 2259+586.

6. Solving the Age Discrepancy

The magnetar 1E 2259+586 is located nearly at the very center of the half-moon-shaped shell of CTB 109 (section 4.1, figure 1). This coincidence is difficult to explain by invoking a chance superposition of the two objects. We therefore assume that 1E 2259+586 and CTB 109 were indeed produced by the same supernova explosion (section 1.1), while τ_c of 1E 2259+586 is somehow significantly overestimated, compared to its true age which we consider to be close to τ_{SNR} .

6.1. Case with a Constant Magnetic Field

To solve the issue of the suggested overestimate of τ_c after Colpi et al. (2000) and Dall’Osso et al. (2012), let us begin with reviewing the meaning of τ_c . In general, the spin evolution of a pulsar with dipole surface magnetic field B is expressed empirically as

$$\frac{d\omega}{dt} = -bB^2\omega^n \quad (4)$$

with $b \equiv 32\pi^3 R_{\text{psr}}^6 / 3I\mu_0 c^3$ and the braking index of $n = 3$, where $R_{\text{psr}} = 10 \text{ km}$ is the pulsar’s radius, $I = 9.5 \times 10^{44} \text{ g cm}^2$ its momentum of inertia, μ_0 vacuum permeability and c the light velocity. If we use the pulse period $P = 2\pi/\omega$ and its derivative \dot{P} instead of ω and $\dot{\omega}$, equation (4) becomes

$$B = \sqrt{\frac{P\dot{P}}{b}} \simeq 3.2 \times 10^{19} \sqrt{P\dot{P}} \text{ G}. \quad (5)$$

If B does not depend on time t , equation (4) can be integrated as

$$t = -\frac{1}{n-1} \left(\frac{\omega}{\dot{\omega}} \right) \left[1 - \left(\frac{\omega}{\omega_0} \right)^{n-1} \right] = \tau_c \left[1 - \left(\frac{\omega}{\omega_0} \right)^{n-1} \right] \quad (6)$$

where ω and $\dot{\omega}$ both refer to the present values, while ω_0 is the angular frequency at $t = 0$ (i.e. the birth). Assuming that $(\omega/\omega_0)^{n-1}$ can be neglected, the characteristic age is defined as

$$\tau_c \equiv \frac{\dot{\omega}}{(n-1)\omega} \equiv \frac{P}{(n-1)\dot{P}}. \quad (7)$$

These equations are generally used for pulsars, and found in some textbooks (e.g., Lyne & Graham-Smith 1998).

More generally, the true age of the pulsar, denoted by t_0 , can be compared with its τ_c as

$$\frac{\tau_c}{t_0} = \frac{1}{1 - \left(\frac{\omega}{\omega_0}\right)^{n-1}} = \frac{1}{1 - \left(\frac{P_0}{P}\right)^{n-1}} \simeq 1 + \left(\frac{P_0}{P}\right)^{n-1}, \quad (8)$$

where $P_0 = 2\pi/\omega_0$, and the last expression is the first-order approximation in $(P_0/P)^{n-1}$. Thus, τ_c becomes somewhat larger than t_0 if $(P_0/P)^{n-1}$ cannot be neglected. Conversely, if we somehow have an independent estimate of t_0 its comparison with τ_c can be used to infer P_0 as

$$P_0 = P \left(-\frac{t_0}{\tau_c} + 1 \right)^{1/(n-1)}. \quad (9)$$

For example, the Crab pulsar (Staelin & Reifenstein, 1968), with $P = 33$ ms, $\dot{P} = 2.42 \times 10^{-13}$ ss $^{-1}$ and $n = 2.509$ (Lyne et al., 1993), has $\tau_c = 1241$ yr. Comparing this with its true age of 960 yr (as of 2014), equation (9) yields $P_0 = 18$ ms if assuming $n = 2.509$, on $P_0 = 15.7$ ms if $n = 3.0$ (for ideal magnetic dipole radiation). Thus, regardless of the employed value of n , the small difference between τ_c and t_0 of the Crab pulsar can be understood to imply that it has so far lost $\sim 3/4$ of its initial rotational energy in ~ 1 kyr.

In contrast to the above case of young active pulsars, we would need to invoke $P_0 = P \times 0.97 = 6.76$ s, if equation (9) with $n = 3$ were used to explain the large discrepancy, $\tau_c/t_0 \sim \tau_c/\tau_{\text{SNR}} \sim 16$, found in the CTB/1E2259+586 system. This would lead to a view that 1E 2259+586 was born some 14 kyr ago as a slow rotator of which the spin period is much longer than those (0.2 s to 2 s) of the majority of *currently* observed (hence relatively old) radio pulsars, and has so far lost only a tiny fraction of its rotational energy in 14 kyr. However, such a view is opposite to a general consensus that new-born magnetars must be rotating rapidly, even faster than ordinary pulsars, in order for them to acquire the strong magnetic fields (e.g., Usov 1992, Duncan & Thompson 1996, Lyons et al. 2010). Furthermore, an NS with $P_0 = 6.67$ s, has an angular momentum of only $\sim 10^{-5}$ of those of typical new-born pulsars with $P_0 \sim 10$ ms including the Crab pulsar, and hence would require an extreme fine tuning in the progenitor-to-NS angular momentum transfer during the explosion. We therefore conclude that the age problem of 1E2259+586 cannot be solved as long as its magnetic field is assumed to have been constant since its birth.

6.2. Effects of Magnetic Field Decay

Since the age problem of 1E 2259+586/CTB 109 cannot be solved as long as B is considered constant, we may next examine the case where B decays with time (section 1.1). In fact, the X-ray emission of magnetar is thought to arise when their magnetic energies are consumed (Thompson & Duncan, 1995). Then, the calculations presented in section 5.1 would be no longer valid, and we need to integrate equation (6) considering the time evolution of B .

Let us consider a simple magnetic field decay model employed by Colpi et al. (2000), namely

$$\frac{dB}{dt} = -aB^{1+\alpha}, \quad (10)$$

where $\alpha \geq 0$ is a parameter, and a is another positive constant. This equation can be solved as

$$B(t) = \begin{cases} \frac{B_0}{\left(1 + \frac{\alpha t}{\tau_d}\right)^{1/\alpha}} & (\alpha \neq 0) \\ B_0 \exp\left(\frac{-t}{\tau_d}\right) & (\alpha = 0) \end{cases} \quad (11)$$

where B_0 represents the initial value of B , and $\tau_d = (1/aB_0^\alpha)$, an arbitrary constant, means a typical lead time till the power-law like decay of B begins.

Substituting equation (11) into equation (4), we can derive P as a function of t . Then, as already given by Dall'Osso et al. (2012), τ_c can be expressed as a function of t , P_0 , α and τ_d as

$$\tau_c = \begin{cases} \frac{\tau_d}{2-\alpha} \left[\left\{ 1 + (2-\alpha) \frac{\tau_0}{\tau_d} \right\} \left(1 + \frac{\alpha t}{\tau_d} \right)^{2/\alpha} - \left(1 + \frac{\alpha t}{\tau_d} \right) \right] & (\alpha \neq 0, 2) \\ \frac{\tau_d}{2} \left[\left(1 + \frac{2\tau_0}{\tau_d} \right) \exp\left(\frac{2t}{\tau_d}\right) - 1 \right] & (\alpha = 0) \\ \left(1 + \frac{2t}{\tau_d} \right) \left[\tau_0 + \frac{\tau_d}{2} \ln\left(1 + \frac{2t}{\tau_d} \right) \right] & (\alpha = 2) \end{cases} \quad (12)$$

where $\tau_0 \equiv P_0/2\dot{P}_0$ is the initial value of τ_c . The first form of equation (12) reduces to equation (8) for $\alpha \rightarrow \infty$ or $\tau_d \rightarrow \infty$, i.e., the case of a constant B .

6.3. Magnetic Field Evolution of 1E 2259+586

Our next task is to examine whether the observed values of P and \dot{P} of 1E 2259+586 can be explained with the picture presented in section 6.2. Equation (12) involves four free parameters, namely α , B_0 , τ_d and P_0 , whereas we have only two observables, P and \dot{P} at $t = t_0 \simeq 14$ kyr. In section 5.1, we showed that the effect of P_0 can be neglected, when the current P is long enough. Therefore, we chose to fix P_0 at 3 ms where strong dynamo works efficiently (e.g., Duncan & Thompson 1996). To visualize effects of P_0 , another solution with $P_0 = 10, 100$ ms and $\alpha = 1.2$ is also shown in figure 3 [panels (b), (c), and (d)]. Thus, the effects of P_0 are limited to very early ($\ll 1$ s) stages of the evolution, and its value does not affect our discussion as long as it is much shorter than ~ 6.7 s.

Then, if α is specified, we can find a pair (B_0, τ_d) that can simultaneously explain P and \dot{P} at present. Figure 3 shows the behavior of such a family of solutions to equation (12). Below, we try to constrain the values of α (hence of B_0 and τ_d), assuming that α is relatively common among magnetars. This is because the broad-band X-ray spectra of magnetars are determined rather uniquely by τ_c (Enoto et al., 2010), so that τ_c is considered to be tightly related to t_0 even if these two are unlikely to be identical: object-to-object scatter in α would cause a scatter in the τ_c/t_0 ratio, and would make the relation of Enoto et al. (2010) difficult to interpret.

When α is small ($0 \leq \alpha < 0.5$), the field would decay, as seen in equation (10), either exponentially (if $\alpha = 0$) on a time scale of τ_d , or if $\alpha \neq 0$, with a relatively steep power-law after a long lead time $\tau_d \sim t_0$. The required initial field, $B_0 \sim 10^{15}$ G, is reasonable. However, the implied view would be rather ad-hoc: 1E 2259+586 had been relatively inactive until recently, when it suddenly started to release its magnetic energy with a high rate. Furthermore, if such a small value of α were common to magnetars, their age differences would make, as in figure 3 (a), their present-day field distribution scatter much more widely than is observed. Hence we regard these small values of α unlikely.

As α increases towards 2.0, the power-law field decay becomes milder, with shorter values of τ_d and stronger initial fields B_0 . The implication is that the object started releasing its magnetic energy rather soon after the birth, and had already dumped away a large fraction of its rotational energy at a very early stage when the field was still very strong. As seen in figure 3 (c), the spin period has almost converged to its terminal value (see also Dall’Osso et al. 2012). Therefore, this case can explain the observed narrow scatter in P of magnetars, assuming that they share relatively similar values of α and B_0 . However, the cases with $\alpha \sim 2.0$ or larger would require too strong initial fields, e.g., $B_0 \sim 10^{17}$ G, which would be much higher than the strongest dipole field observed from magnetars, $B = 2.4 \times 10^{15}$ G of SGR 1806–20 (Nakagawa et al. 2009). Therefore, such large- α solutions are unlikely, too.

To summarize these examinations, figure 3 (e) shows the locus of the allowed solutions on the (α, τ_d) plane, where the values of B_0 are also indicated. We thus reconfirm the above considerations, that the range of $1 \lesssim \alpha < 2$ is appropriate, in agreement with the suggestion by Dall’Osso et al. (2012). Some discussions follow in subsection 7.1.

7. Discussion

7.1. Comparison with Other Objects

We reconfirmed the age problem of 1E 2259+586 and CTB 109, and presented a way to solve it with a simple magnetic field decay model. The result agrees with the basic concept of magnetar hypothesis which implies that the energies stored by their magnetic fields should be consumed to supply their X-ray luminosities exceeding those available with their spin down. The amount of released field energies can be reflected in the overestimations of the characteristic ages.

Let us then examine whether this concept applies to other NS/SNR associations, including both magnetars and ordinary pulsars. Figure 4 shows relations between τ_c of such single pulsars and the ages of their host SNRs. Data points of ordinary pulsars are distributed around the line representing $\tau_c/\tau_{\text{SNR}} = 1$ with a few exceptions (e.g., Torii et al. 1999 for J1811–1925/G11.2–0.3). Therefore, radio pulsars, including the particular case of the Crab pulsar (section 6.1), are considered to be free from the age problem.

In addition to the ordinary pulsars, figure 4 shows a few other magnetar/SNR associations. The magnetar CXOU J171405.7-381031 has a very small characteristic age of 0.96 kyr (Sato et al., 2010),

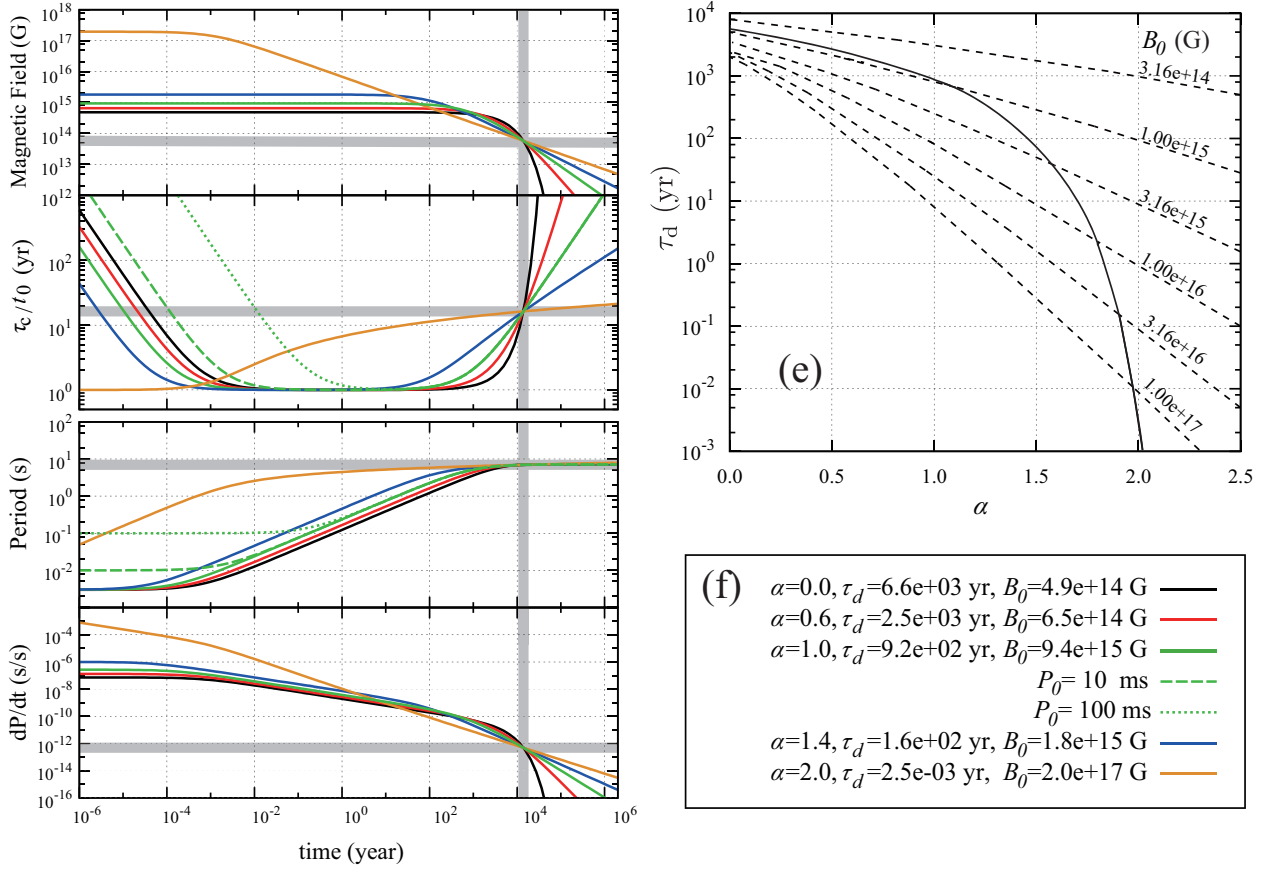


Fig. 3. Possible evolution tracks of 1E 2259+586 assuming equation (4) and equation (10). Panels (a)-(d) represent the behavior of the magnetic field B , the over-estimation factor of the characteristic age (i.e., τ_c/t_0), the pulse period P , and its time derivative \dot{P} , respectively. The six representative tracks are all constrained to reproduce the presently measured P and \dot{P} at $t = 14$ kyr. The dashed and dotted ones assume $P_0 = 10$ ms and 100 ms, respectively, while the other five all $P_0 = 3$ ms. Panel (e) shows the trajectory of solutions that can explain the present-day ($t = 14$ kyr) 1E 2259+586. Dashed lines indicate the initial field value B_0 . Panel (f) summarizes the parameter sets of the trajectories.

which is consistent, within rather large errors, with the age ($0.65_{-0.3}^{+2.5}$ kyr; Nakamura et al. 2009) the associated SNR, CTB 37B. Another magnetar/SNR association, 1E 1841-045/Kes73, is located in figure 4 between J171405.7-381031/CTB 37B and 1E 2259+586/CTB 109. The age of Kes73 was estimated by Kumar et al. (2014), as $0.75 - 2.1$ kyr (table 4). Combining this with $\tau_c = 4.7$ kyr of 1E 1841-045 (table 4), the age discrepancy of this pair becomes $\tau_c/\tau_{\text{SNR}} = 2.7 - 8$. These two associations do not show large overestimation factors of τ_c/τ_{SNR} as much as 1E 2259+586/CTB 109 association. Thus, the three magnetar/SNR associations (including 1E 2259+586/CTB 109) suggest that the age over-estimation factor, τ_c/τ_{SNR} , increases towards older objects. This agrees, at least qualitatively, with the theoretical behavior seen in figure 3 (c), as long as P_0 is negligible.

We hence tried to explain the data points of these three magnetar/SNR associations with a common set of parameters, and derive a plausible range of α . For this purpose, three evolution tracks representing the solutions to equation (12) for 1E 2259+586/CTB 109 are additionally plotted on

figure 4. Each parameter set is the same as that of figure 3(f). If α is small as $0 \leq \alpha < 0.6$ (dashed red line), the CXOU J171405.7-381031/CTB 37B association cannot be explained. On the other hand, large value of $\alpha (> 1.5)$ fail to explain the 1E 1841-045/Kes73 association. Thus, the three magnetar/SNR pairs in figure 4 can be explained in a unified way if they have a common value of α (and also of τ_d) that is in the range of $0.6 < \alpha < 1.4$.

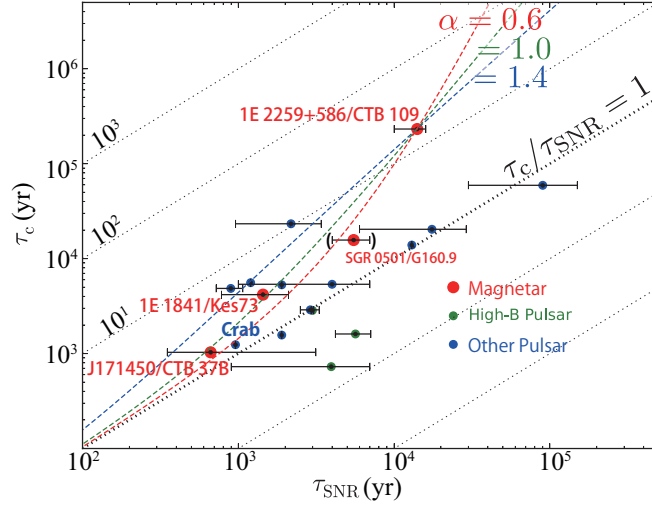


Fig. 4. Relations between τ_{SNR} and τ_c of single NSs associated with SNRs. Red, magenta and blue represent magnetars, high-B pulsars and rotation powered pulsars, respectively. Parameters are listed in table 4. The SGR 0501+4516/G160.9+2.6 pair is parenthesized, because the association is rather doubtful, and this SNR might be associated to another pulsar PSR B0458+46 (e.g., Leahy & Roger 1991). The red, green, and blue dashed curves indicate solutions to equation (12), with $(\alpha, \tau_d, B_0) = (0.6, 2.5 \times 10^3 \text{ yr}, 6.5 \times 10^{14} \text{ G})$, $(1.0, 9.2 \times 10^2 \text{ yr}, 9.4 \times 10^{15} \text{ G})$ and $(1.4, 1.6 \times 10^2 \text{ yr}, 1.8 \times 10^{15} \text{ G})$, respectively. They all assume $P_0 = 3 \text{ ms}$, and B_0 which is specified by figure 3 (e).

7.2. Supporting Evidence

The scenario so far developed implies that magnetars form a population that is much younger than previously thought. This important inference is supported by an independent piece of evidence. Figure 5 shows a spatial distribution of NSs including magnetars. Because of steady motions after kick velocities are given by explosions, older pulsars with larger τ_c are thus distributed up to farther distances from the Galactic plane. In contrast, magnetars are much more concentrated to the plane for their nominal age, as better seen in figure 5 (b) which is a projection of figure 5 (a) along the direction perpendicular to the Galactic plane. This implies two possible scenarios; magnetars, as we have shown, are much younger than indicated by their τ_c , or their kick velocities are systematically lower than those of others. Recently, proper motions of four magnetars (SGR 1806–20, SGR 1900+14, 1E 2259+586 and 4U 0142+61) were successfully measured by Tendulkar et al. (2012, 2013). They calculated the mean and standard deviation of their ejection velocities as 200 km s^{-1} and 90 km s^{-1} ,

respectively. They also conclude that the weighted average velocity of magnetars is in good agreement with the tangential velocities of the pulsar population (Hobbs et al., 2005). Therefore, we are left with the former of the two possibilities. In other words, magnetars should be systematically younger than ordinary pulsars that have similar τ_c .

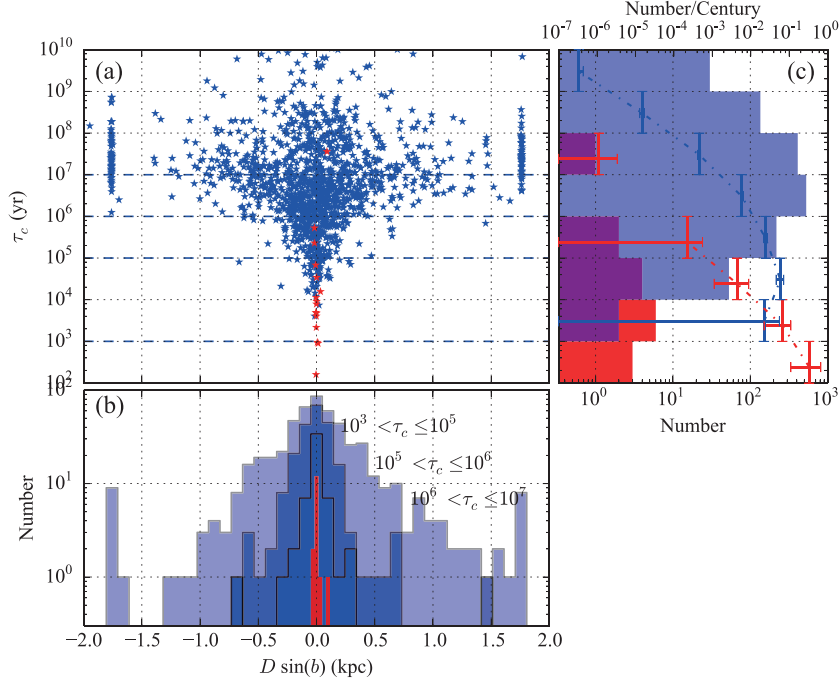


Fig. 5. (a) Spatial distributions of magnetars (red) and radio pulsars (blue). Abscissa and ordinate means distance from the Galactic plane and characteristic age, respectively. (b) Projection of panel (a) onto the direction perpendicular to the Galactic plane. Radio pulsars are divided into three subgroups according to their age. (c) Age distributions of the objects, produced by projecting panel (a) onto the time axis. Histograms represent numbers of pulsars with ages in that logarithmic interval, while crosses tied by a dotted line show the object number per century.

7.3. Implication for the Magnetar Population

Observationally, magnetars are no longer a minority of NS species. This is shown in figure 5 (c), which is the projection of figure 5 (a) onto the time axis. Thus, even if τ_c is not corrected for the over estimation, magnetars already occupy a considerable fraction of young NSs. If we replace τ_c of magnetars with their true ages, their dominance among young NSs will become even more enhanced.

As yet another important implication, we expect that numerous aged magnetar descendants would lurk in our Galaxy. Radio pulsars, observed as the major population of NSs, cannot harbor such aged magnetars, because their P are shorter than those of magnetars. Instead, such objects may be being discovered as weak-field SGRs, including SGR 0418+5729 (Rea et al., 2013), Swift J1822.31606 (Rea et al. 2012; Scholz et al. 2012) and 3XMM J185246.6+003317 (Zhou et al., 2014).

8. Summary

We performed 4 pointings observations of CTB 109 with Suzaku. The spectra extracted from eastern parts of the SNR were well fitted with two plasma components having two different temperatures. Assuming thermal equilibrium between electrons and protons, the shock velocity was calculated as 460 km s^{-1} , and the age of the SNR was estimated as 14 kyr using the Sedov-similarity solution. These results are consistent with the conclusion of the previous work by Sasaki et al. (2013). We thus reconfirmed the huge discrepancy between the age of CTB 109 and the characteristic age of 1E 2259+586.

We consider that the characteristic age of 1E 2259+586 is significantly overestimated, as compared to its true age which we identify with that of CTB109. This effect, seen also in some other magnetars to a lesser extent, can be attributed to decay of their magnetic fields, as implied by the basic concept of “magnetars”. In fact, the observed pulse period and its derivative of 1E 2259+586 has been explained successfully by a family of solutions to a simple equation describing the magnetic field decay. Furthermore, the τ_c vs τ_{SNR} relations of the three magnetar-SNR associations, including the 1E 2259+586/CTB 109 pair, can be explained consistently if they have a common value of α in the range of 0.6-1.4. As a result, magnetars are considered to be much younger than was considered so far, and are rather dominant among new-born NSs. The youth of magnetars is supported independently by their much stronger concentration along the Galactic plane than ordinary pulsars.

Table 4. Parameters for Figure 4.

#	Pulsar/SNR	P (ms)	\dot{P} (ss ⁻¹)	B ($\times 10^{12}$ G)	τ_c (kyr)	τ_{SNR} (kyr)
1	1E 1841-045/Kes73	11778	4.5×10^{-11}	730	4	0.75 - 2.1
2	SGR 0501+4516/G160.9+2.6	5762	5.8×10^{-12}	190	16	4 - 7
3	J171405.7-381031/CTB37B	3824	5.9×10^{-11}	480	0.96	$0.65^{+25}_{-0.3}$
4	1E 2259+586/CTB 109*	6979	4.8×10^{-13}	58	230	10 - 16
5	J1846-0258/Kes75	326	7.1×10^{-12}	49	0.7	0.9 - 4.3
6	J1119-6127/G292.2-0.5	407	4.0×10^{-12}	41	1.6	4.2 - 7.1
7	J1124-5916/G292.0+1.8	135	7.5×10^{-13}	10	2.9	2.93 - 3.05
8	J1513-5908/G320.4-1.2	151	1.5×10^{-12}	15	1.6	1.9
9	J0007+7303/G119.5+10.2	315	3.6×10^{-13}	11	14	13
10	J1930+1852/G54.1+0.3	136	7.5×10^{-13}	10	2.9	2.5 - 3.3
11	J1856+0113/W44	267	2.1×10^{-13}	7.5	20	6 - 29
12	J0633+0632/G205.5+0.5	297	8.0×10^{-14}	4.9	60	30 - 150
13	Crab	33	4.2×10^{-13}	3.8	1.2	0.959
14	J0205+6449/3C 58	65	1.9×10^{-13}	3.6	5	1-7
15	J1833-1034/G21.5-0.9	61	2.0×10^{-13}	3.6	5	0.72 - 1.07
16	J1747-2809/G0.9+0.1	52	1.6×10^{-13}	2.9	5	1.9
17	J1813-1749/G12.8-0.0	44	1.3×10^{-13}	2.4	6	1.2
18	J1811-1925/G11.2-0.3	64	4.4×10^{-14}	1.7	2.3	0.96 - 3.4

* This work.

Data for P and \dot{P} of pulsar were collected from ATNF Pulsar catalogue (Manchester et al., 2005)¹

Data for τ_{SNR} were collected from Ferrand & Safi-Harb (2012)²

References

- Allen, M. P., & Horvath, J. E. 2004, *ApJ*, 616, 346
- Baykal, A., Swank, J. H., Strohmayer, T., & Stark, M. J. 1998, *A&A*, 336, 173
- Camilo, F., Ransom, S. M., Halpern, J. P., & Reynolds, J. 2007, *ApJ*, 666, L93
- Castro, D., Slane, P., Ellison, D. C., & Patnaude, D. J. 2012, *ApJ*, 756, 88
- Chevalier, R. A. 2005, *ApJ*, 619, 839
- Chevalier, R. A. 2011, *American Institute of Physics Conference Series*, 1379, 5
- Coe, M. J., & Jones, L. R. 1992, *MNRAS*, 259, 191
- Coe, M. J., Jones, L. R., & Lehto, H. 1994, *MNRAS*, 270, 178
- Colpi, M., Geppert, U., & Page, D. 2000, *ApJ*, 529, L29

¹ <http://www.atnf.csiro.au/research/pulsar/psrcat>

² <http://www.physics.umanitoba.ca/snr/SNRcat>

- Dall'Osso, S., Granot, J., & Piran, T. 2012, MNRAS, 422, 2878
- Davies, S.R., Coe, M.J., Payne, B.J., & Hanson, C. G. 1989, MNRAS, 237, 973
- Duncan, R. C., & Thompson, C. 1992, ApJ, 392, L9
- Duncan, R. C., & Thompson, C. 1996, High Velocity Neutron Stars, 366, 111
- Enoto, T., Nakazawa, K., Makishima, K., Rea, N., Hurley, K., & Shibata, S. 2010, ApJ, 722, L162
- Enoto, T., et al. 2010, PASJ, 62, 475
- Esposito, P., et al. 2010, The Astronomer's Telegram, 2691, 1
- Fahlman, G. G., & Gregory, P. C. 1983, Supernova Remnants and their X-ray Emission, 101, 445
- Fahlman, G. G., Gregory, P. C., Middleditch, J., Hickson, P., & Richer, H. B. 1982, ApJ, 261, L1
- Ferrand, G., & Safi-Harb, S. 2012, Advances in Space Research, 49, 1313
- Gaensler, B. M. 2004, Advances in Space Research, 33, 645
- Gavriil, F. P., & Kaspi, V. M. 2002, ApJ, 567, 1067
- Gavriil, F. P., Kaspi, V. M., & Woods, P. M. 2004, X-ray Timing 2003: Rossi and Beyond, 714, 302
- Ghavamian, P., Laming, J. M., & Rakowski, C. E. 2007, ApJ, 654, L69
- Gregory, P. C., & Fahlman, G. G. 1980, Nature, 287, 805
- Göğüş, E., Woods, P. M., Kouveliotou, C., Kaneko, Y., Gaensler, B. M., Chatterjee, S. 2010, ApJ, 722, 899
- Hanson, C. G., Dennerl, K., Coe, M. J., & Davis, S. R. 1988, A&A, 195, 114
- Heydari-Malayeri, M., Kahane, C., & Lucas, R. 1981, Nature, 293, 549
- Heyl, J. S., & Hernquist, L. 1999, MNRAS, 304, L37
- Hobbs, G., Lorimer, D. R., Lyne, A. G., & Kramer, M. 2005, MNRAS, 360, 974
- Hughes, V. A., Harten, R. H., & van den Bergh, S. 1981, ApJ, 246, L127
- Hulleman, F., van Kerkwijk, M. H., Verbunt, F. W. M., & Kulkarni, S. R. 2000, A&A, 358, 605
- Igoshev, A. P. 2012, Electromagnetic Radiation from Pulsars and Magnetars, 466, 207
- Ishisaki, Y., et al. 2007, PASJ, 59, 113
- Iwasawa, K., Koyama, K., & Halpern, J. P. 1992, PASJ, 44, 9
- Kaspi, V. M., Chakrabarty, D., & Steinberger, J. 1999, ApJ, 525, L33
- Kaspi, V. M., Gavriil, F. P., & Woods, P. M. 2002, The Astronomer's Telegram, 99, 1
- Kothes, R., & Foster, T. 2012, ApJ, 746, L4
- Kothes, R., Uyaniker, B., & Yar, A. 2002, ApJ, 576, 169
- Koyama, K., Hoshi, R., & Nagase, F. 1987, PASJ, 39, 801
- Koyama, K. et al. 1989, PASJ, 41, 461
- Koyama, K., et al. 2007, PASJ, 59, 23
- Kumar, H. S., Safi-Harb, S., Slane, P. O., & Gotthelf, E. V. 2014, IAU Symposium, 296, 235
- Leahy, D. A., & Roger, R. S. 1991, AJ, 101, 1033
- Lyne, A.G., Pritchard, R. S., & Graham-Smith, F. 1993, MNRAS, 265, 1003
- Lyne, A. G., & Graham-Smith, F. 1998, Pulsar astronomy / Andrew G. Lyne and Francis Graham-Smith. Cambridge, U.K.; New York : Cambridge University Press, 1998. (Cambridge astrophysics series ; 31) ISBN 0521594138,

Lyons, N., O'Brien, P. T., Zhang, B., Willingale, R., Troja, E., Starling, R. L. C. 2010, MNRAS, 402, 705

Manchester, R. N., Hobbs, G. B., Teoh, A., & Hobbs, M. 2005, AJ, 129, 1993

McKee, C. F., & Ostriker, J. P. 1977, ApJ, 218, 148

Mereghetti, S., Israel, G. L., & Stella, L. 1998, MNRAS, 296, 689

Nakamura, R., Bamba, A., Ishida, M., Nakajima, H., Yamazaki, R., Terada, Y., Phlhofer, G., Wagner, S.J. 2009, PASJ, 61, 197

Pandey, U. S. 1996, A&A, 316, 111

Rea, N., et al. 2010, Science, 330, 944

Rea, N., Israel, G. L., Esposito, P., et al. 2012, ApJ, 754, 27

Rea, N., et al. 2013, ApJ, 770, 65

Safi-Harb, S., & Kumar, H. S. 2013, IAU Symposium, 291, 480

Sasaki, M., Kothes, R., Plucinsky, P. P., Gaetz, T. J., & Brunt, C. M. 2006, ApJ, 642, L149

Sasaki, M., Plucinsky, P. P., Gaetz, T. J., & Bocchino, F. 2013, A&A, 552, A45

Sasaki, M., Plucinsky, P. P., Gaetz, T. J., Smith, R. K., Edgar, R. J., 2004, ApJ, 617, 322

Sato, T., Bamba, A., Nakamura, R., & Ishida, M. 2010, PASJ, 62, L33

Sedov, L. I. 1959, Similarity and Dimensional Methods in Mechanics, New York: Academic Press, 1959,

Seward, F. D. 1985, Comments on Astrophysics, 11, 15

Shull, J. M., & van Steenberg, M. 1982, ApJS, 48, 95

Sofue, Y., Takahara, F., & Hirabayashi, H. 1983, PASJ, 35, 447

Staelin, D. H., & Reifenstein, E. C., III 1968, Science, 162, 1481

Scholz, P., Ng, C.-Y., Livingstone, M. A., et al. 2012, ApJ, 761, 66

Tatematsu, K., Fukui, Y., Nakano, M., Kogure, T., Ogawa, H., & Kawabata, K. 1987, A&A, 184, 279

Tatematsu, K., Nakano, M., Yoshida, S., Wiramihardja, S. D., & Kogure, T. 1985, PASJ, 37, 345

Taylor, G. 1950, Royal Society of London Proceedings Series A, 201, 159

Tendulkar, S. P., Cameron, P. B., & Kulkarni, S. R. 2012, ApJ, 761, 76

Tendulkar, S. P., Cameron, P. B., & Kulkarni, S. R. 2013, ApJ, 772, 31

Thompson, C., & Duncan, R. C. 1995, MNRAS, 275, 255

Torii, K., Tsunemi, H., Dotani, T., Mitsuda, K., Kawai, N., Kinugasa, K., Saito, Y., & Shibata, S. 1999, ApJ, 523, L69

Usov, V. V. 1992, Nature, 357, 472

Usov, V. V. 1994, ApJ, 427, 984

Vink, J. 2008, Advances in Space Research, 41, 503

Vink, J., & Kuiper, L. 2006, MNRAS, 370, L14

Woods, P. M., et al. 2004, X-ray Timing 2003: Rossi and Beyond, 714, 298

Zhou, P., Chen, Y., Li, X.-D., Safi-Harb, S., Mendez, M., Terada, Y., W. & Ge, M.-Y. 2014, ApJ, 781, L16